Histomorphometric Evaluation of Non-Thermal Plasma-Treated Xenogenic Bone Graft for Enhanced Bone Regeneration in a Rabbit Calvarial Defect Model: Part I

Hyunsuk Choi , Yong-Suk Moon , Hyung-Gyun Kim , Dong-Seok Sohn *

Posted Date: 23 April 2026

doi: 10.20944/preprints202604.1617.v1

Keywords: non-thermal plasma treatment; xenograft; bone regeneration; histomorphometric analysis; rabbit calvarial defect

 doi:10.20944/preprints202604.1617.v1

Article

Histomorphometric Evaluation of Non-Thermal Plasma-Treated Xenogenic Bone Graft for Enhanced Bone Regeneration in a Rabbit Calvarial Defect Model: Part I

Hyunsuk Choi [1], Yong-Suk Moon [2], Hyung-Gyun Kim [3] and Dong-Seok Sohn [4,*]

[1] Department of Dentistry and Prosthodontics, Daegu Catholic University School of Medicine, Daegu 42472, Republic of Korea
[2] Department of Anatomy, Daegu Catholic University School of Medicine, Daegu 42472, Republic of Korea
[3] Department of Dentistry and Advanced General Dentistry, Daegu Catholic University School of Medicine, Daegu 42472, Republic of Korea
[4] Department of Dentistry and Oral and Maxillofacial Surgery, Daegu Catholic University School of Medicine, Daegu 42472, Republic of Korea
* Correspondence: dssohn@cu.ac.kr; Tel.: +82-53-650-4288; Fax: +82-53-622-7067

Abstract

When placing dental implants, xenografts are most commonly used clinically to compensate for insufficient bone volume of patients. However, xenografts have limitations including low osteoinductive capacity and prolonged healing time. The aim of this study was to evaluate the effects of non-thermal plasma-treated bovine cancellous bone graft on new bone formation, graft resorption, bone marrow formation, and vascularization in a rabbit calvarial defect model. Twenty-four adult male New Zealand white rabbits received bilateral 8-mm critical-size calvarial defects. One defect was filled with untreated SANTA-OSS® (control) and the contralateral defect with plasma-treated SANTA-OSS using the ACTILINK™ Reborn device. Animals were sacrificed at 2, 4, and 8 weeks (n=8 per group) for histomorphometric analysis. The plasma-treated group showed significantly higher new bone area (14.12 ± 0.69%, 18.93 ± 0.68%, and 32.72 ± 0.61% at 2, 4, and 8 weeks) than the control at all time points ($p < 0.05$). In addition, the experimental group exhibited accelerated graft resorption, larger bone marrow area, greater blood vessel area, and more TRAP-positive osteoclasts compared with the control ($p < 0.05$). Within the limitations of this study, plasma treatment significantly enhanced new bone formation, accelerated graft resorption, promoted bone marrow development, and increased vascularization.

Keywords: non-thermal plasma treatment; xenograft; bone regeneration; histomorphometric analysis; rabbit calvarial defect

1. Introduction

Dental implants have been a widely used treatment for lost teeth [1]. However, in cases of alveolar bone defects caused by various factors such as periodontal disease, inflammation, or alveolar bone atrophy, the width or height of the bone is often insufficient for implant placement [2]. In such cases, alveolar bone grafting is frequently used in dental clinical practice, either simultaneously with or prior to implant placement [3].

The purpose of alveolar bone graft materials is to induce and promote the regenerative capacity of alveolar bone. Bone regeneration is broadly categorized into osteogenesis, osteoinduction, and osteoconduction [4]. Osteogenesis is the process of new bone formation and development, occurring when the cells within the grafted bone material themselves proliferate bone. Osteoinduction is a

 doi:10.20944/preprints202604.1617.v1

method that induces bone regeneration by utilizing bone-forming proteins or other growth factors that trigger osteoinduction stimulation. Osteoconduction is a method in which the bone graft material fills the bone defect, acting as a connecting structure for bone formation [5,6].

Autologous bone graft materials possess all three of the aforementioned mechanisms and have long been regarded as the gold standard for dental bone graft treatment due to their advantages of excellent biocompatibility and freedom from immune reactions. However, autologous bone has drawbacks, such as the need for additional donor sites, risks of trauma or infection during harvesting, limited harvesting volume, and potential pain at the harvesting site and a prolonged healing period [7].

Allogeneic and xenogeneic bone grafts have also been widely used as alternatives to autologous bone grafts. These materials have the advantages of being readily available in large quantities, eliminating the need for additional surgery at the donor site, and maintaining structural stability as a scaffold to fill bone defects. Among them, bovine-derived cancellous bone xenografts, which possess a structure similar to human bone, are the most frequently used in clinical practice. However, these xenografts have limitations, including low osteoinductive capacity, a risk of immune reactions or infection, and the need for a long healing period before they are completely replaced by new bone formation [8,9].

To overcome the limitations of existing xenograft materials, various surface modification technologies have been studied to enhance the biological performance of the grafts [10]. Recently, in the field of dental clinical practice, the method of treating implant surfaces or alveolar bone graft materials with non-thermal atmospheric pressure plasma has been attracting attention [11]. Plasma, the fourth state of matter, is created by applying high voltage to gases such as O_2, Ar, and N_2 to generate reactive oxygen and nitrogen species. When this plasma is applied to the surface of bone graft materials or titanium implants, it can effectively remove hydrocarbon contaminants accumulated during the biological aging process [11]. Furthermore, as the contact angle approaches 0°, superhydrophilicity is restored, facilitating the adsorption of proteins such as fibronectin and albumin, and significantly enhancing cell adhesion, proliferation, and differentiation [10,11]. These modifications promote the initial bone formation process, increase alkaline phosphatase (ALP) activity, and stimulate angiogenesis and new bone formation without altering the original surface morphology of the graft material [11,12].

Previous in vitro and in vivo studies have shown that treating the surface of implant fixtures with plasma improves blood compatibility and reduces oxidative stress, thereby accelerating osseointegration [13]. Furthermore, results indicate that plasma treatment prevents the stability dip phenomenon—where implant stability decreases after placement—allowing for a rapid recovery of stability [14].

While there has been some research on plasma surface treatment for implants as described above [13,14], its application to xenografts remains limited. Studies on plasma-treated bone grafts are scarce, and comprehensive histomorphological evaluations in standardized defect models are still lacking [15].

Therefore, the aim of this study was to evaluate the effects of non-thermal plasma-treated bovine cancellous bone graft on new bone formation, graft resorption, bone marrow formation, and vascularization in a rabbit calvarial defect model. This study represents Part I of a companion series, in which histomorphometric analysis was performed. The immunohistochemical analysis of osteogenic and angiogenic markers will be reported separately in Part II.

2. Materials and Methods

2.1. Experimental Materials

In this study, bovine-derived cancellous bone graft (SANTA-OSS®, BIOTEM Co., Ltd., Korea) and the ACTILINK™ Reborn non-thermal atmospheric pressure plasma device (Plasmapp Co., Ltd., Daejeon, Korea) were used. Plasma activation of the SANTA-OSS surface was performed

 doi:10.20944/preprints202604.1617.v1

immediately before implantation using the ACTILINK™ Reborn device. Each graft underwent two consecutive 1-minute treatment cycles according to the manufacturer's protocol [16]. This chairside plasma treatment effectively removes surface hydrocarbon contaminants and restores superhydrophilicity without altering the original topography of the graft particles.

2.2. Surgical Procedures

Twenty-four adult male New Zealand white rabbits weighing 2.8–3.2 kg (average 3.0 kg) were used. All experimental procedures were approved by the Institutional Animal Care and Use Committee of Daegu Catholic University Medical Center (approval number: DCIAFCR-240620-12-Y). The rabbits were randomly assigned to three healing-period groups (2, 4, and 8 weeks; n = 8 per group). General anesthesia was induced with an intramuscular injection of ketamine (30 mg/kg, Ketalar; Yuhan Co., Seoul, Korea) and xylazine (10 mg/kg, Rompun; Bayer Korea, Seoul, Korea). Additionally, 0.5 mL of lidocaine with 1:100,000 epinephrine was injected subcutaneously along the midline of the calvaria. After skin and periosteal incision along the sagittal midline, two circular critical-size defects (8 mm diameter) were created in the frontal bone using an 8-mm trephine burr. The resected bone discs were carefully removed without damaging the underlying dura. In each animal, one defect was filled with 0.5 cc of untreated SANTA-OSS (control group) and the contralateral defect was filled with 0.5 cc of plasma-treated SANTA-OSS (experimental group) (figure 1). The periosteum and skin were sutured with 4-0 nylon (Blue nylon, Ailee Co., Busan, Korea). All animals received intramuscular gentamicin (20 mg/kg, Donghwa Co., Seoul, Korea) for 3 days postoperatively. The rabbits were sacrificed at 2 weeks (n = 8), 4 weeks (n = 8), or 8 weeks (n = 8) after surgery.

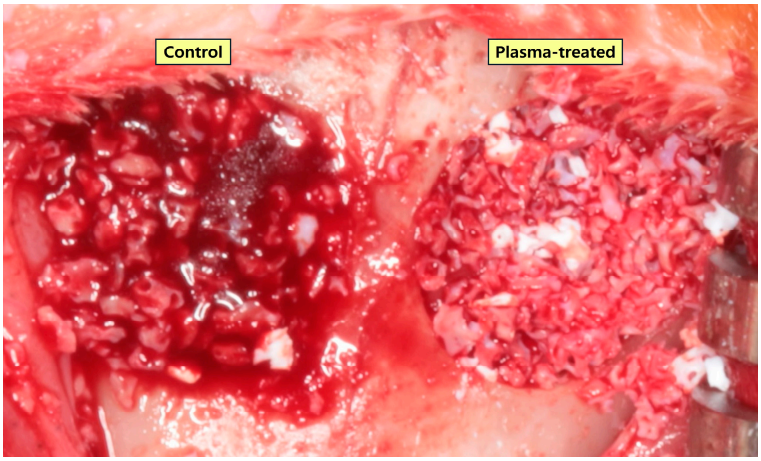

Figure 1. Application of bone graft materials in the rabbit calvarial defects. Left: untreated SANTA-OSS (Control group); Right: non-thermal plasma-treated SANTA-OSS (Experimental group).

2.3. Tissue Preparation

At the designated time points (2, 4, and 8 weeks), the animals were sacrificed under general anesthesia. The calvarial specimens were harvested using a microsaw, fixed in 10% neutral buffered formalin for 24 hours, washed with 0.1 M phosphate buffer solution, and decalcified in 10% formic acid for 10 days. After decalcification, the specimens were embedded in paraffin (Paraplast; Oxford, USA) and serially sectioned at 5 μm thickness through the center of each defect. The sections were stained with hematoxylin-eosin (H&E) and Masson's trichrome (MT) for histological evaluation of new bone formation and soft tissue changes.

 doi:10.20944/preprints202604.1617.v1

2.4. Histomorphometric Analysis

Ten randomly selected fields from each specimen were photographed at ×20 and ×200 magnification using an Axiophot photomicroscope (Carl Zeiss, Germany) equipped with an AxioCam MRc5 camera (Carl Zeiss, Germany). Histomorphometric measurements were performed using AxioVision SE64 software (Carl Zeiss, Germany). The following parameters were quantified as percentages of the total augmented area:

- Newly formed bone area
- Remaining graft material area
- Soft tissue area
- Bone marrow area
- Blood vessel area

The total augmented area included newly formed bone, residual graft particles, fibrous/soft tissue, bone marrow, and vascular structures within the original 8-mm defect boundaries.

2.5. Tartrate-Resistant Acid Phosphatase (TRAP) Staining

Tartrate-resistant acid phosphatase (TRAP) activity was detected using an acid phosphatase kit (Sigma-Aldrich, St. Louis, MO, USA) according to the manufacturer's instructions. Paraffin-embedded sections were cleared, dehydrated, and incubated for 1 hour at 37 °C in the dark with a mixture containing naphthol AS-BI phosphate (25 mg), fast garnet GBC salt (15 mg), and 27 mmol tartaric acid in 0.1 mol acetate buffer (pH 5.2). The sections were counterstained with acid hematoxylin and mounted. Slides were examined under an Axiophot photomicroscope with AxioVision SE64 software. For each slide, twenty fields were randomly selected, and the number of TRAP-positive multinucleated osteoclasts (dark brown) was counted in a standardized 1 mm^2 area of the augmented region.

2.6. Statistical Analysis

Data are expressed as mean ± standard error. Statistical analyses were performed using SPSS software (version 25.0, IBM Corp., Chicago, IL, USA). Differences between the control and experimental groups at each time point, as well as differences among healing periods within each group, were evaluated by one-way analysis of variance (ANOVA) followed by Tukey's post-hoc test. A p-value < 0.05 was considered statistically significant.

3. Results

3.1. Histological Analysis

SANTA-OSS particles were lightly stained and clearly distinguished from the surrounding tissues in both hematoxylin-eosin (H&E) and Masson's trichrome (MT) stains. Lamellar host bone stained red, whereas woven or newly formed bone stained blue in MT stain. No signs of inflammation were observed in either the control or experimental group under light microscopy. In all specimens, the center of the defect remained level without depression, and the SANTA-OSS particles maintained the space-maintaining property.

At 2 weeks, new bone formation was limited to the defect margins in both groups, although the amount of newly formed bone differed markedly between groups. By 4 weeks, the thickness and density of newly formed bone had increased compared with the 2-week specimens. At 8 weeks, abundant new bone was observed along the defect margins and around the graft particles in both groups (Figure 2–5).

In the control group, newly formed bone at 2 weeks was confined to the defect margins and graft surfaces, with osteoblasts lining the newly formed bone (Figure 2a, 3a, 4a, 5a). At 4 weeks, bone thickness and density had increased, yet bone formation remained predominantly at the margins, while graft particle density decreased (Figure 2c, 3c, 4c, 5c). At 8 weeks, new bone on graft surfaces

 doi:10.20944/preprints202604.1617.v1

had further increased, but only a small amount reached the defect center; bone marrow spaces began to appear between new bone and residual graft particles (Figure 2e, 3e, 4e, 5e).

In the experimental group (plasma-treated SANTA-OSS), new bone formation at 2 weeks was already observed extending toward the defect center. Newly formed bone covered the surfaces of plasma-treated graft particles and extended into the intervening connective tissue, with numerous osteoblasts present (Figure 2b, 3b, 4b, 5b). At 4 weeks, bone thickness and density were markedly greater than at 2 weeks, with some new bone reaching the defect center; notably, numerous large and small blood vessels were evident within the connective tissue (Figure 2d, 3d, 4d, 5d). At 8 weeks, new bone thickness and density were substantially higher than at 4 weeks. Graft particle size and density had decreased further, and prominent bone marrow spaces containing adipose tissue were observed between the newly formed bone trabeculae (Figure 2f, 3f, 4f, 5f).

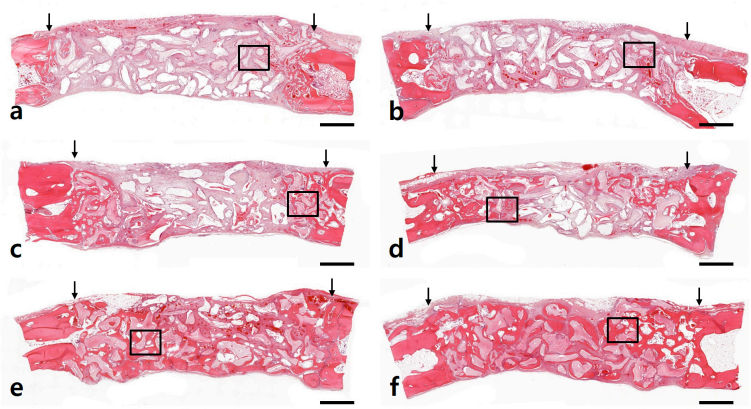

Figure 2. Low-magnification images (x20) of the rabbit calvaria after surgery at 2 weeks (a), 4 weeks (c), and 8 weeks (e) in the control group, and at 2 weeks (b), 4 weeks (d), and 8 weeks (f) in the experimental group. The arrows indicate the margins of the defect. The boxed areas are presented at higher magnification in Fig. 3. Hematoxylin-eosin stain (Scale bar: 1000 μm).

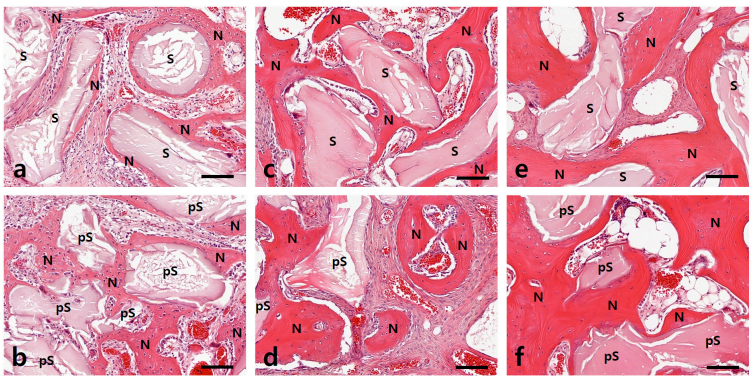

Figure 3. Higher-magnification images (x200) showing the new bone formation after surgery at 2 weeks (a), 4 weeks (c), and 8 weeks (e) in the control group, and at 2 weeks (b), 4 weeks (d), and 8 weeks (f) in the experimental group. N, newly formed bone; s, SANTA-OSS particles; ps, plasma-treated SANTA-OSS particles. Hematoxylin-eosin stain (Scale bar: 100 μm).

 doi:10.20944/preprints202604.1617.v1

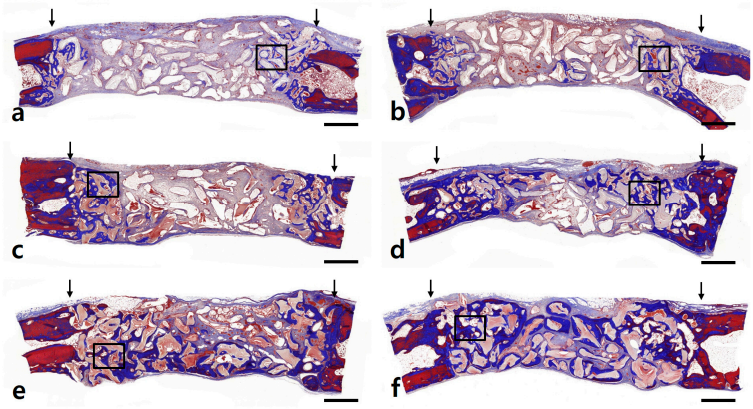

Figure 4. Low-magnification images (x20) of the rabbit calvaria after surgery at 2 weeks (a), 4 weeks (c), and 8 weeks (e) in the control group, and at 2 weeks (b), 4 weeks (d), and 8 weeks (f) in the experimental group. The arrows indicate the margins of the defect. The boxed areas are presented at higher magnification in Fig. 5. Masson's trichrome stain (Scale bar: 1000 μm).

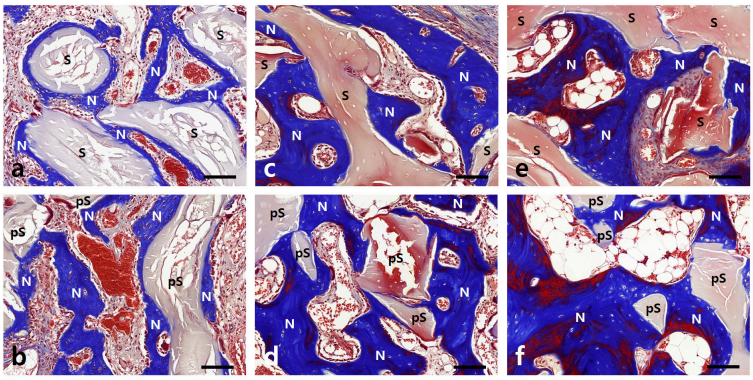

Figure 5. Higher-magnification images (x200) showing the new bone formation after surgery at 2 weeks (a), 4 weeks (c), and 8 weeks (e) in the control group, and at 2 weeks (b), 4 weeks (d), and 8 weeks (f) in the experimental group. N, newly formed bone; s, SANTA-OSS particles; ps, plasma-treated SANTA-OSS particles. Masson's trichrome stain (Scale bar: 100 μm).

3.2. Histomorphometric Analysis

The percentage of newly formed bone area relative to the total augmented area in the control group was 7.85 ± 0.46%, 14.44 ± 0.44%, and 23.41 ± 0.68% at 2, 4, and 8 weeks, respectively. In the experimental group, the corresponding values were 14.12 ± 0.69%, 18.93 ± 0.68%, and 32.72 ± 0.61%. One-way ANOVA with Tukey's post-hoc test revealed that new bone area at 8 weeks was significantly greater than at 2 and 4 weeks in both groups ($p < 0.05$). Furthermore, the percentage of newly formed bone was significantly higher in the experimental group than in the control group at all time points (Figure 6).

 doi:10.20944/preprints202604.1617.v1

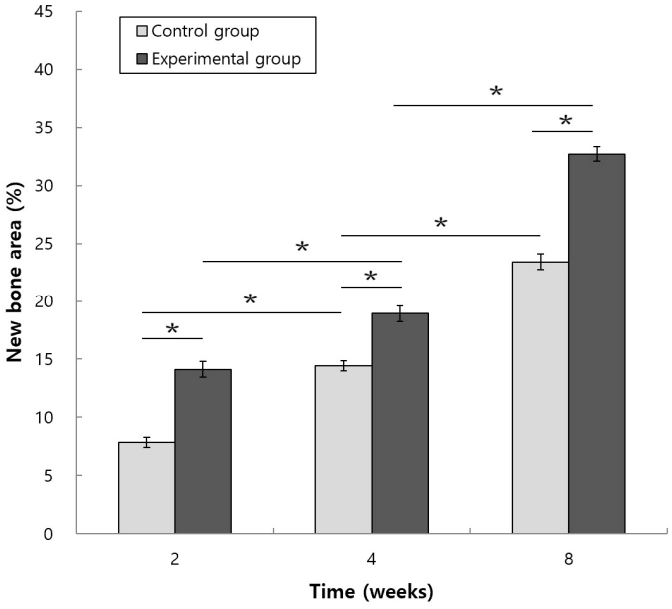

Figure 6. Histomorphometric measurement of the area of newly formed bone to the area of the total augmented area at 2, 4, and 8 weeks in the control group and experimental group. (*P < 0.05).

The percentage of remaining graft material area in the control group was 40.72 ± 0.53%, 36.42 ± 0.64%, and 33.77 ± 0.67% at 2, 4, and 8 weeks, respectively. In the experimental group, the values were 35.71 ± 1.04%, 34.90 ± 0.75%, and 30.93 ± 0.53%. Graft material area at 8 weeks was significantly lower than at 2 weeks in both groups ($p < 0.05$). The remaining graft area was significantly smaller in the experimental group at 2 and 8 weeks compared with the control group (Figure 7).

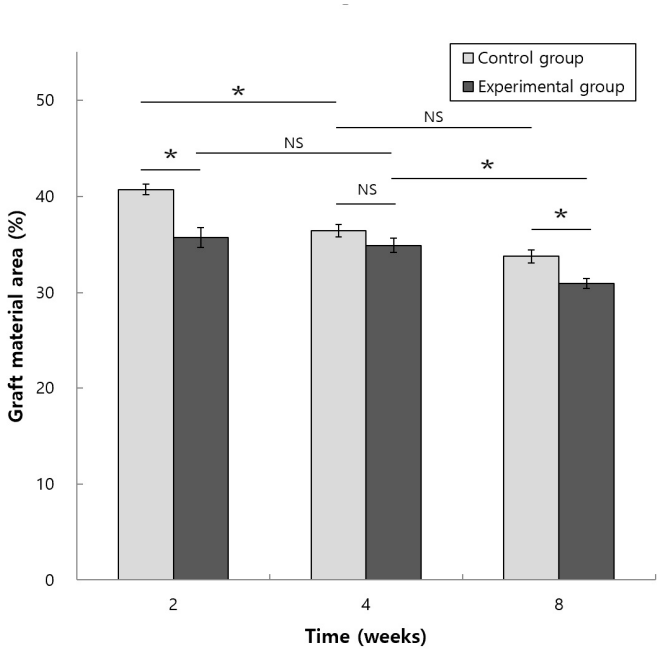

Figure 7. Histomorphometric measurement of the area of graft material to the area of the total augmented area at 2, 4, and 8 weeks in the control group and experimental group. (*P < 0.05).

The percentage of soft tissue area in the control group was 51.43 ± 0.76%, 48.70 ± 0.55%, and 39.00 ± 0.55% at 2, 4, and 8 weeks, respectively. In the experimental group, the values were 50.17 ± 1.21%,

 doi:10.20944/preprints202604.1617.v1

44.15 ± 0.53%, and 29.23 ± 0.71%. Soft tissue area at 8 weeks was significantly lower than at 2 and 4 weeks in both groups ($p < 0.05$). The soft tissue area was significantly smaller in the experimental group at 4 and 8 weeks compared with the control group (Figure 8).

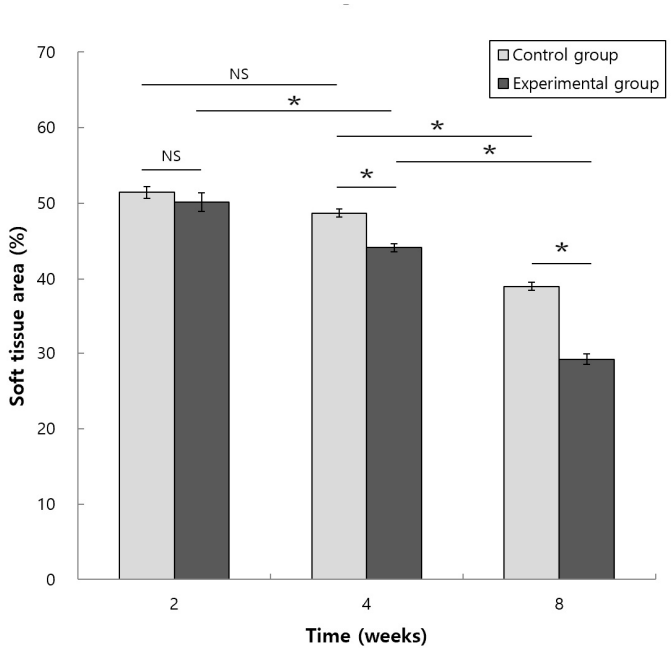

Figure 8. Histomorphometric measurement of the area of soft tissue to the area of the total augmented area at 2, 4, and 8 weeks in the control group and experimental group. (*P < 0.05).

Bone marrow area (measured from 4 weeks onward) in the control group was 0.44 ± 0.17% and 3.82 ± 0.33% at 4 and 8 weeks, respectively. In the experimental group, the values were 2.02 ± 0.26% and 7.12 ± 0.95%. Bone marrow area at 8 weeks was significantly greater than at 4 weeks in both groups ($p < 0.05$). The bone marrow area was significantly larger in the experimental group at 8 weeks compared with the control group (Figure 9).

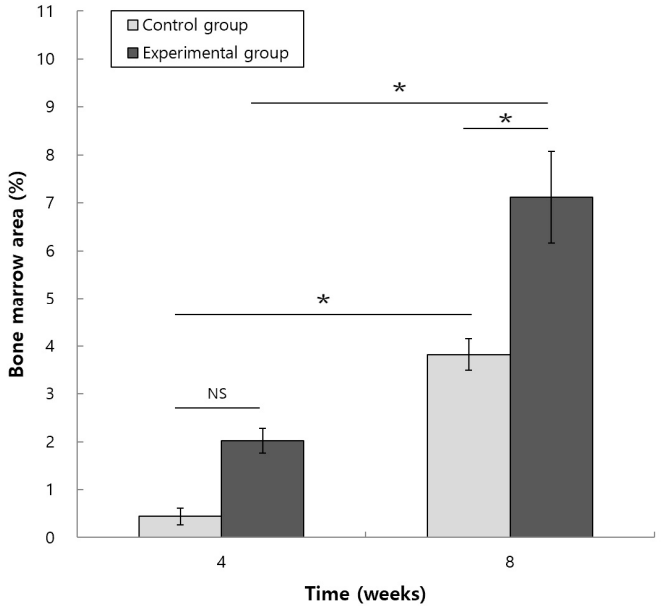

Figure 9. Histomorphometric measurement of the area of bone marrow to the area of the total augmented area at 4 and 8 weeks in the control group and experimental group. (*P < 0.05).

 doi:10.20944/preprints202604.1617.v1

Blood vessel area in the control group was 2.68 ± 0.10%, 7.20 ± 0.43%, and 4.59 ± 0.38% at 2, 4, and 8 weeks, respectively. In the experimental group, the values were 5.35 ± 0.12%, 9.14 ± 0.34%, and 6.65 ± 0.47%. Blood vessel area peaked at 4 weeks and was significantly higher than at 2 and 8 weeks in both groups ($p < 0.05$). The blood vessel area was significantly greater in the experimental group at all time points compared with the control group (Figure 10).

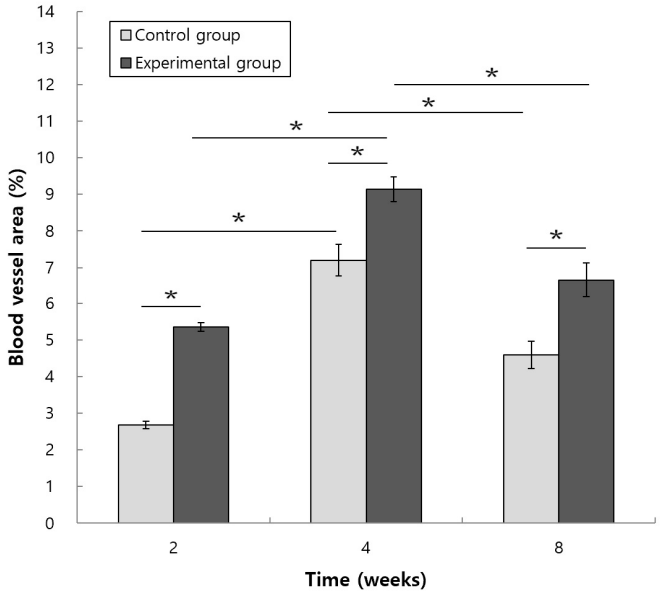

Figure 10. Histomorphometric measurement of the area of blood vessel to the area of the total augmented area at 2, 4, and 8 weeks in the control group and experimental group. (*P < 0.05).

3.3. Tartrate-Resistant Acid Phosphatase (TRAP) Staining

In the control group, TRAP-positive osteoclasts were observed on the surfaces of newly formed bone and SANTA-OSS particles at 2 weeks (Figure 11a). Their number increased at 4 weeks (Figure 11c) and decreased again at 8 weeks (Figure 11e). In the experimental group, numerous TRAP-positive osteoclasts were already present on newly formed bone and plasma-treated SANTA-OSS surfaces at 2 weeks (Figure 11b). The number was highest at 4 weeks (Figure 11d) and decreased at 8 weeks (Figure 11f).

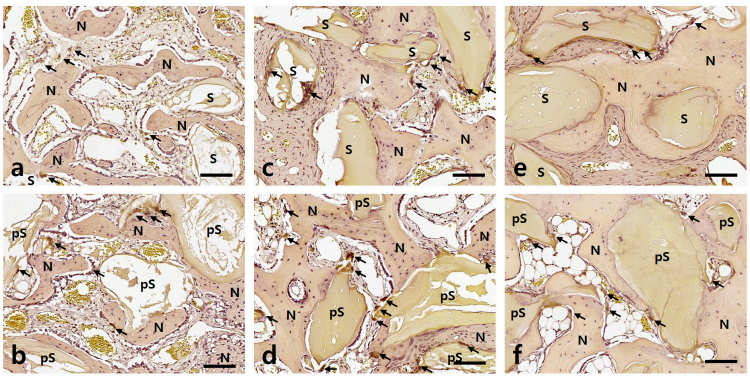

Figure 11. High-magnification images (x200) showing TRAP-stained osteoclasts (arrows) in the control group at 2 weeks (a), 4 weeks (c), and 8 weeks (e), and in the experimental group at 2 weeks (b), 4 weeks (d), and 8 weeks (f). N, newly formed bone; s, SANTA-OSS particles; ps, plasma-treated SANTA-OSS particles (Scale bar: 100 μm).

 doi:10.20944/preprints202604.1617.v1

Quantitatively, the number of TRAP-positive osteoclasts per 1 mm² in the control group was 11.68 ± 0.41, 13.97 ± 0.30, and 11.29 ± 0.41 at 2, 4, and 8 weeks, respectively. In the experimental group, the values were 14.82 ± 0.47, 18.12 ± 0.60, and 13.69 ± 0.53. The number peaked at 4 weeks and was significantly higher than at 2 and 8 weeks in both groups ($p < 0.05$). The number of TRAP-positive osteoclasts was significantly greater in the experimental group at all time points compared with the control group (Figure 12).

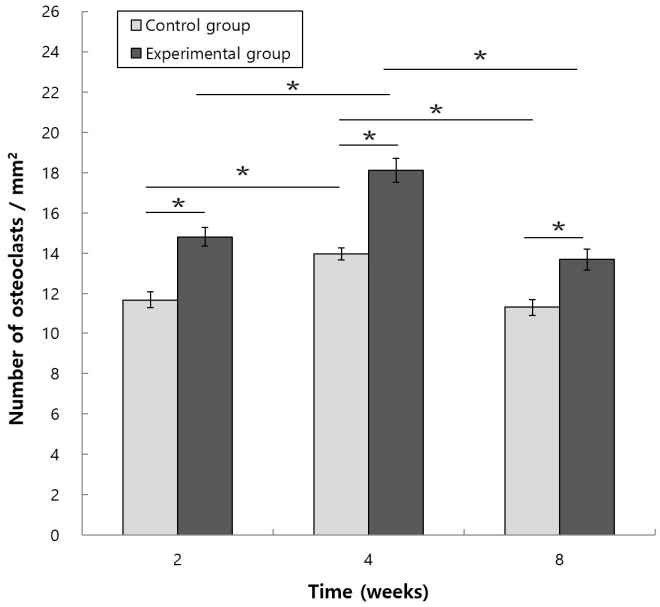

Figure 12. Histomorphometric measurement of the number of TRAP-stained osteoclasts by 1 mm2 of the augmented area at 2, 4, and 8 weeks in the control group and experimental group. (*P < 0.05).

4. Discussion

The experimental results of this study showed that non-thermal atmospheric pressure plasma treatment significantly promotes and enhances new bone formation in a rabbit calvarial defect model. At all observation periods (2, 4, and 8 weeks), the experimental group treated with plasma-treated SANTA-OSS exhibited a larger volume of new bone, faster absorption of the graft material, a wider bone marrow space, and increased angiogenesis compared to the untreated control group. These results suggest that simple plasma treatment using the ACTILINK™ Reborn system in the dental clinic has the potential to significantly improve the osteogenic capacity of bone graft materials [17,18].

In this study, the experimental group demonstrated superior results compared to the control group across all observed indicators; however, the most notable difference was the amount of new bone formation. The plasma-treated group exhibited a significantly higher proportion of new bone compared to the control group throughout all observation periods, and notably, at week 8, the new bone extended to the center of the defect site. This rapid centripetal bone growth is a phenomenon rarely observed within a short period with conventional xenograft materials. Furthermore, the absorption rate of the graft material in the experimental group was faster than that of the control group, and distinct bone marrow spaces containing adipose tissue were observed at week 8. These results suggest that plasma treatment not only promotes bone formation but also induces the balanced remodeling of the graft scaffold, enabling physiological bone marrow formation more rapidly than in the control group [19,20].

In addition, another important finding is that the vascular area in the plasma-treated group significantly increased starting from week 2. Promoting angiogenesis is considered an essential prerequisite for successful bone regeneration because it supplies oxygen, nutrients, and progenitor cells to the defect site [21]. The number of TRAP-positive osteoclasts increased at week 4, supporting

 doi:10.20944/preprints202604.1617.v1

the concept that the graft is reformed more actively by plasma treatment. The pattern of osteoclast activity peaking at week 4 and decreasing at week 8 suggests that the stages of bone resorption and bone formation are efficiently linked, which is essential for mature bone development [22].

The biological mechanisms underlying these improvements are closely related to the well-documented effects of non-thermal plasma on biomaterial surfaces [23,24]. Plasma effectively removes hydrocarbon contaminants that accumulate during storage (biological aging), restores superhydrophilicity, and markedly enhances protein adsorption (fibronectin, albumin, etc.) [23]. These surface changes promote early cell attachment, proliferation, and differentiation of osteogenic cells while reducing oxidative stress and improving hemocompatibility [24]. Although the present study focused on histomorphometry (Part I), the accelerated vascularization and osteoclast activity observed here strongly suggest that plasma treatment creates a more favorable microenvironment for both osteogenesis and angiogenesis—findings that will be further elucidated by immunohistochemical analysis of osteogenic and angiogenic markers in the companion Part II study.

When compared with previous animal studies using biological enhancers, the magnitude of improvement observed in the present study is comparable to that reported by Kim et al. (2025), who demonstrated significantly enhanced new bone formation and graft resorption using mesenchymal stem cell-conditioned media combined with human allogeneic bone in the same rabbit calvarial defect model [14]. In addition, these results are consistent with Tallarico et al. (2025), who reported that vacuum plasma surface treatment significantly improves the hydrophilicity and wettability of bone graft substitutes and resorbable membranes [16]. However, unlike conditioned media which requires complex preparation and raises concerns regarding cost and regulatory issues, the plasma activation used in this study is a simple, immediate chairside physical method that requires no additional biological agents [25]. This suggests that non-thermal plasma treatment may offer a more practical and reproducible alternative for enhancing xenograft performance.

Nevertheless, several limitations should be acknowledged. This study was conducted in a non-loaded calvarial defect model, so the results may not be directly transferable to load-bearing alveolar ridge or sinus augmentation sites in humans. In addition, only three healing periods (2, 4, and 8 weeks) were evaluated; longer-term observations (12–24 weeks) would provide further insight into the final quality and volume of regenerated bone. Finally, although histomorphometry provides reliable quantitative data on bone volume and remodeling, it does not fully elucidate the underlying cellular and molecular mechanisms, which will be addressed in the forthcoming immunohistochemical Part II paper. Taken together, the present findings indicate that plasma treatment markedly enhances the bone regenerative capacity of SANTA-OSS.

5. Conclusions

Within the limitations of this study, non-thermal atmospheric pressure plasma treatment of SANTA-OSS significantly enhanced new bone formation, accelerated graft resorption, promoted bone marrow development, and increased vascularization in the rabbit calvarial defect model. The plasma-treated group exhibited significantly greater new bone area at 2, 4, and 8 weeks ($p < 0.05$), along with more rapid graft resorption, larger bone marrow spaces, and enhanced angiogenesis compared with the control.

This study demonstrated that plasma activation using the ACTILINK™ Reborn system, which is performed simply in the chairside, can significantly enhance the osteogenic capacity of bovine cancellous bone grafts without the need for additional biological agents. Plasma-treated xenografts offer more predictable and rapid bone regeneration, possessing the potential to accelerate implant placement and improve clinical outcomes in alveolar bone augmentation. Further mechanistic insights will be presented in the upcoming immunohistochemistry study (part 2).

Author Contributions: Conceptualization, D.-S.S.; methodology, H.C. and H.-G.K.; software, Y.-S.M.; validation, H.C. and D.-S.S.; formal analysis, Y.-S.M.; investigation, H.-G.K. and D.-S.S.; resources, D.-S.S.; data curation, Y.-S.M.; writing—original draft preparation, H.C.; writing—review and editing, H.C. and D.-S.S.;

 doi:10.20944/preprints202604.1617.v1

visualization, Y.-S.M.; supervision, D.-S.S.; project administration, D.-S.S.; funding acquisition, H.C. All authors have read and agreed to the published version of the manuscript.

Funding: This work was supported by the grant of Research Institute of Medical Science, Daegu Catholic University (2024).

Institutional Review Board Statement: The animal study protocol was approved by the Institutional Animal Care and Use Committee of Daegu Catholic University Medical Center (approval number: DCIAFCR-240620-12-Y).

Informed Consent Statement: Not applicable.

Data Availability Statement: The original contributions presented in this study are included in the article. Further inquiries can be directed to the corresponding author.

Acknowledgments: During the preparation of this manuscript/study, the author(s) used generative AI tools were used solely for language editing and clarity improvement. No AI systems were used for data generation, analysis, interpretation, or study design. The authors have reviewed and edited the output and take full responsibility for the content of this publication.

Conflicts of Interest: The authors declare no conflicts of interest.

References

1. Findler, M.; Chackartchi, T.; Rimbach, S.; Mann, J.; Tobias, G. Clinical Success Rates of Dental Implants with Bone Grafting in a Large-Scale National Dataset. J Funct Biomater. 2026, 17, 46. https://doi.org/10.3390/jfb17010046
2. Elboraey, M.O.; Alqutaibi, A.Y.; Aboalrejal, A.N.; Borzangy, S.; Zafar, M.S.; Al-Gabri, R.; Alghauli, M.A.; Ramalingam, S. Regenerative approaches in alveolar bone augmentation for dental implant placement: Techniques, biomaterials, and clinical decision-making: A comprehensive review. J Dent. 2025, 154, 105612. https://doi.org/10.1016/j.jdent.2025.105612
3. Yu, S.H.; Saleh, M.H.A.; Wang, H.L. Simultaneous or staged lateral ridge augmentation: A clinical guideline on the decision-making process. Periodontol 2000. 2023, 93, 107-128. https://doi.org/10.1111/prd.12512
4. Wang, H.; Kang, J. Bone grafts and synthetic substitutes in dental applications. Front Bioeng Biotechnol. 2026, 13, 1759864. https://doi.org/10.3389/fbioe.2025.1759864
5. Ferraz, M.P. Bone Grafts in Dental Medicine: An Overview of Autografts, Allografts and Synthetic Materials. Materials. 2023, 16, 4117. https://doi.org/10.3390/ma16114117
6. Nicolae, C.L.; Pîrvulescu, D.C.; Niculescu, A.G.; Epistatu, D.; Mihaiescu, D.E.; Antohi, A.M.; Grumezescu, A.M.; Croitoru, G.A. An Up-to-Date Review of Materials Science Advances in Bone Grafting for Oral and Maxillofacial Pathology. Materials. 2024, 17, 4782. https://doi.org/10.3390/ma17194782
7. Heimes, D.; Pabst, A.; Becker, P.; Hartmann, A.; Kloss, F.; Tunkel, J.; Smeets, R.; Kämmerer, P.W. Comparison of morbidity-related parameters between autologous and allogeneic bone grafts for alveolar ridge augmentation from patients' perspective-A questionnaire-based cohort study. Clin Implant Dent Relat Res. 2024, 26, 170-182. https://doi.org/10.1111/cid.13242
8. Ciszyński, M.; Dominiak, S.; Dominiak, M.; Gedrange, T.; Hadzik, J. Allogenic Bone Graft in Dentistry: A Review of Current Trends and Developments. Int J Mol Sci. 2023, 24, 16598. https://doi.org/10.3390/ijms242316598
9. Zhang, J.; Zhang, W.; Yue, W.; Qin, W.; Zhao, Y.; Xu, G. Research Progress of Bone Grafting: A Comprehensive Review. Int J Nanomed. 2025, 20, 1875-1895. https://doi.org/10.2147/IJN.S510524
10. Makary, C.; Menhall, A.; Lahoud, P.; Yang, K.R.; Park, K.B.; Razukevicius, D.; Traini, T. Bone-to-Implant Contact in Implants with Plasma-Treated Nanostructured Calcium-Incorporated Surface (XPEEDActive) Compared to Non-Plasma-Treated Implants (XPEED): A Human Histologic Study at 4 Weeks. Materials. 2024, 17, 2331. https://doi.org/10.3390/ma17102331

 doi:10.20944/preprints202604.1617.v1

11. Schafer, S.; Swain, T.; Parra, M.; Slavin, B.V.; Mirsky, N.A.; Nayak, V.V.; Witek, L.; Coelho, P.G. Nonthermal Atmospheric Pressure Plasma Treatment of Endosteal Implants for Osseointegration and Antimicrobial Efficacy: A Comprehensive Review. Bioengineering. 2024, 11, 320. https://doi.org/10.3390/bioengineering11040320
12. Fischer, M.; Bortel, E.; Schoon, J.; Behnke, E.; Hesse, B.; Weitkamp, T.; Bekeschus, S.; Pichler, M.; Wassilew, G.I.; Schulze, F. Cold physical plasma treatment optimization for improved bone allograft processing. Front Bioeng Biotechnol. 2023, 11, 1264409. https://doi.org/10.3389/fbioe.2023.1264409
13. Barausse, C.; Tayeb, S.; Pellegrino, G.; Sansavini, M.; Mancuso, E.; Mazzitelli, C.; Felice, P. Cold Plasma Treatment on Titanium Implants and Osseointegration: A Systematic Review. Appl. Sci. 2025, 15, 10302. https://doi.org/10.3390/app151910302
14. Kim, Y.-K.; Choi, H.; Kim, H.-G.; Sohn, D.-S. Impact of Plasma Surface Treatment on Implant Stability and Early Osseointegration: A Retrospective Cohort Study. Materials. 2025, 18, 4568. https://doi.org/10.3390/ma18194568
15. Stacchi, C.; Rapani, A.; Montanari, M.; Martini, R.; Lombardi, T. Effect of Vacuum Plasma Activation on Early Implant Stability: a Single-Blind Split-Mouth Randomized Clinical Trial. J Oral Maxillofac Res. 2025, 16, e4. https://doi.org/10.5037/jomr.2025.16205
16. Tallarico, M.; Meloni, S.M.; Troia, M.; Cacciò, C.; Lumbau, A.I.; Gendviliene, I.; Ceruso, F.M.; Pisano, M. The Use of Vacuum Plasma Surface Treatment to Improve the Hydrophilicity and Wettability of Bone Graft Substitutes and Resorbable Membranes: An In Vitro Study. Dent. J. 2025, 13, 141. https://doi.org/10.3390/dj13040141
17. Wu, C.; Ma, K.; Zhao, H.; Zhang, Q.; Liu, Y.; Bai, N. Bioactive effects of nonthermal argon-oxygen plasma on inorganic bovine bone surface. Scientific reports. 2020, 10, 17973. https://doi.org/10.1038/s41598-020-75195-2
18. Shimatani, A.; Toyoda, H.; Orita, K.; Hirakawa, Y.; Aoki, K.; Oh, J. S.; Shirafuji, T.; Nakamura, H. In vivo study on the healing of bone defect treated with non-thermal atmospheric pressure gas discharge plasma. PloS one. 2021, 16, e0255861. https://doi.org/10.1371/journal.pone.0255861
19. Ahn, J.-J.; Yoo, J.-H.; Bae, E.-B.; Kim, G.-C.; Hwang, J.J.; Lee, W.-S.; Kim, H.-J.; Huh, J.-B. The Effects of Atmospheric Pressure Argon Plasma Treated Bovine Bone Substitute on Bone Regeneration. Coatings. 2019, 9, 790. https://doi.org/10.3390/coatings9120790
20. Akçay, H.; Ercan, U.K.; Bahçeci, S.; Ulu, M.; Ibiş, F.; Enhoş, Ş. The Effect of Atmospheric Pressure Cold Plasma Application on Titanium Barriers: A Vertical Bone Augmentation. J Craniofac Surg. 2020, 31, 2054–2058. https://doi.org/10.1097/SCS.0000000000006643
21. Arndt, S.; Unger, P.; Berneburg, M.; Bosserhoff, A.-K.; Karrer, S. Cold atmospheric plasma (CAP) activates angiogenesis-related molecules in skin keratinocytes, fibroblasts and endothelial cells and improves wound angiogenesis in an autocrine and paracrine mode. J Dermatol Sci. 2018, 89, 181-190. https://doi.org/10.1016/j.jdermsci.2017.11.008
22. Xiang, Q.; Li, L.; Ji, W.; Gawlitta, D.; Walboomers, X.F.; van den Beucken, J.J.J.P. Beyond resorption: osteoclasts as drivers of bone formation. Cell Regen. 2024, 13, 22. https://doi.org/10.1186/s13619-024-00205-x
23. Zheng, Z.; Ao, X.; Xie, P.; Wu, J.; Dong, Y.; Yu, D.; Wang, J.; Zhu, Z.; Xu, H. H. K.; Chen, W. Effects of novel non-thermal atmospheric plasma treatment of titanium on physical and biological improvements and in vivo osseointegration in rats. Sci Rep. 2020, 10, 10637. https://doi.org/10.1038/s41598-020-67678-z
24. Kahm, S.H.; Lee, S.H.; Lim, Y.; Jeon, H.J.; Yun, K.-I. Osseointegration of Dental Implants after Vacuum Plasma Surface Treatment In Vivo. J Funct Biomater. 2024, 15, 278. https://doi.org/10.3390/jfb15100278
25. Nonnenmacher, L.; Fischer, M.; Haralambiev, L.; Bekeschus, S.; Schulze, F.; Wassilew, G. I.; Schoon, J.; Reichert, J.C. Orthopaedic applications of cold physical plasma. EFORT Open Rev. 2023, 8, 409–423. https://doi.org/10.1530/EOR-22-0106